The *S. aureus* serine protease-like protein B (SplB) is a potent allergen causing eosinophilic airway inflammation in mice

Jessica von Fournier[1], Christopher Saade[1], Hannes Wolfgramm[2], Marques L. Schilling[1], Shenja Buchholz[3], Susanne Neumeister[1], Yves Laumonnier[4], Henry J. McSorley[5], Leif Steil[2], Matthias Sendler[3], Uwe Völker[2], Murthy N. Darisipudi[1], Barbara M. Bröker[1]

[1] Institute of Immunology, University Medicine Greifswald, Greifswald, Germany

[2] Department of Functional Genomics, University Medicine Greifswald, Greifswald, Germany

[3] Department of Medicine A, University Medicine Greifswald, Greifswald, Germany

[4] Institute for Nutritional Medicine, University of Lübeck, Lübeck, Germany

[5] School of Life Sciences, University of Dundee, Dundee, UK

Keywords: Allergy, asthma, *Staphylococcus aureus*, sensitization, serine protease, virulence factor, immune escape

Abstract

Asthma is a chronic inflammatory disease associated with increased *Staphylococcus aureus* airway colonization. However, the causal relationship is unknown. *S. aureus* secretes several virulence factors that promote allergic sensitization. These include the serine protease-like protein (Spl) B, a secreted protease that elicits a type 2-biased immune response in humans. We studied the allergenic properties of SplB in a mouse model of chronic allergic airway inflammation (AAI). We induced AAI by repeated intratracheal inoculations of recombinant SplB in C57BL/6J mice, wild-type, Rag2 ko, IL-33 ko, and PAR2 ko. We also exposed wild-type mice to an enzymatically inactive mutant of SplB. Airway inflammation was assessed by flow cytometry and airway hyperreactivity measurements. The specific antibody response was characterized by ELISA. We observed severe eosinophil inflammation in the airways and lungs of SplB-sensitized mice, as well as airway hypersensitivity and high SplB-specific serum

IgE titers. Remarkably, SplB induced this asthma phenotype without the need for adjuvants. Characterization of the pathomechanisms revealed that the proteolytic activity of SplB and a functional adaptive immune system were essential for the development of murine asthma. The soluble protease sensor IL-33 was necessary for eosinophil tissue invasion, whereas the membrane-bound protease sensor PAR2 was dispensable. Based on these results, we propose a new mechanism to explain the relationship between *S. aureus* colonization and asthma: *S. aureus* itself can cause allergic airway inflammation via its potent allergen SplB.

Introduction

Asthma is one of the most common chronic inflammatory lung diseases, with over 260 million patients worldwide[1]. Patients suffer from wheezing, coughing, chest tightness and shortness of breath. Asthma is a heterogenous disease, and clinicians differentiate between several asthma phenotypes, of which allergic asthma is the most common[2]. Allergic asthma is characterized by a T helper type 2 cell (Th2) immune response and is triggered by the inhalation of airborne allergens; however, the causes of asthma development are debated[3].

Colonization by certain pathogens is suspected to play a role in asthma development and/or exacerbation, among them *Staphylococcus (S.) aureus*[4]. *S. aureus* is a Gram-positive opportunistic pathogen that permanently colonizes 30% of the adult human population, preferably in the nasopharynx and on the skin[5]. Colonization with *S. aureus* is positively correlated with asthma and also associated with other atopic diseases like atopic dermatitis and chronic rhinosinusitis[6,7]. *S. aureus* is infamous for its potent virulence factors, some of which have been linked to a Th2 response in humans, such as some enterotoxins and the serine protease-like proteins (Spls)[8].

Spls are a group of secreted proteases (commonly named SplA-SplF) that are encoded on the νSaβ genomic island[9–11]. They act as virulence factors as shown in a mouse sepsis model, where infection with an *S. aureus* strain that expressed Spls but no other secreted protease resulted in increased mortality[12]. Moreover, SplD and F cause asthma in an acute asthma mouse model[13]. There is evidence that Spls also modulate the human immune response to *S. aureus*. The antibody response elicited by the Spls is skewed towards IgE and IgG4 in healthy individuals[14]. In asthmatics, the Spl-specific IgE antibody titers are increased[14]. Also, patients with cystic

fibrosis, who are commonly colonized and often chronically infected with *S. aureus*, show strong serum IgE binding to the Spls[15]. The Spls further elicit Th2-biased cellular immune responses in humans[15]. However, the mechanisms underlying the Spl-specific shift towards type 2 immunity are unknown.

The immune response towards prominent human asthma allergens like house dust mite (HDM), pollen and cockroach is well-defined[16–18]. Many of these allergens contain proteases, which provoke a Th2 immune response by cleaving tight junction proteins and activating cell-surface protease sensors, such as the protease activated receptor 2 (PAR2)[19–23]. Moreover, several protease allergens cleave interleukin (IL)-33, an alarmin that is secreted by epithelial cells upon cellular stress and cell death[24]. We aimed to characterize the allergic response towards the potent *S. aureus* protease SplB, with a focus on IL-33 and PAR2, two important sensors of allergic asthma.

Two mutually non-exclusive scenarios have been proposed to explain the association between *S. aureus* colonization and asthma: (1) the Th2 immune response that characterizes asthma facilitates *S. aureus* colonization and (2) *S. aureus* colonization creates a Th2 microenvironment that promotes allergic sensitization towards harmless antigens[8].

To shed light on the interplay between *S. aureus* and airway allergy, we have studied the *S. aureus* protease SplB. We show here that SplB acts as a potent allergen in a mouse model of chronic allergic airway inflammation (AAI). SplB causes severe eosinophilic inflammation on its own without adjuvant. The development of asthma depends on the adaptive immune system and on SplB's protease activity. IL-33 is necessary, but PAR2 is not. Therefore, we propose a third scenario for the relationship between *S. aureus* and asthma: (3) *S. aureus* secretes allergens that can trigger asthma development and exacerbation.

Results

SplB acts as a potent allergen and induces murine AAI

First, we established a sensitization protocol using four intratracheal (i.t.) applications of SplB at different doses in female C57BL/6J wild-type mice (Fig. 1A). Mice treated with PBS served as negative control. Unlike PBS-treated mice, SplB-treated mice exhibited increased airway

hyperreactivity (AHR) upon methacholine challenge, which was largely dose-independent (Fig. 1B). At the highest dose (50 µg/application) SplB induced a significant influx of cells into the lung lumen, as measured in the bronchoalveolar lavage (BAL) (Fig. 1C; gating strategies are provided in Fig. S1-4). These were primarily eosinophils, with only very few neutrophils and $CD4^+$ T cells (Fig. 1D-F). In the lung tissue, SplB induced a similar phenotype, characterized by strong recruitment of eosinophils and $CD4^+$ T cells, but almost no neutrophils (Fig. 1G-J). Notably, the recruited T cells were primarily effector T cells (Fig 1K). The total numbers of dendritic cells (DCs) and all analyzed DC subsets were also significantly higher in the lungs of the SplB-treated mice than in the controls (Fig 1L, M). In the sera of all SplB-treated mice, we observed high SplB-specific IgE titers, which peaked on day 14 and decreased by day 24 (Fig. 1N).

This clearly shows that SplB acts as a potent allergen in our mouse model of chronic AAI. The observed phenotype was largely independent of the administered SplB dose. In general, however, greater interindividual differences were observed in mice treated with 10 µg of SplB per dose than in those treated with 25 µg. Therefore, the following experiments were conducted using 25 µg/application, unless stated otherwise.

SplB-induced AAI depends on an intact adaptive immune system

Certain allergens are known to cause an inflammatory response independently of the adaptive immune system, by activating innate lymphoid cells 2[25]. To ascertain whether a functional adaptive immune system is necessary for the development of SplB-induced AAI, we treated Rag2 ko mice, which lack mature B and T cells, with SplB and compared their phenotype with that of SplB-sensitized wilde-type (WT) mice. Only WT mice responded to SplB with an influx of inflammatory cells into their airways and lungs (Fig. 2A-C). We conclude that an intact adaptive immune system is necessary for the development of SplB-mediated AAI.

The allergenicity of SplB depends on its catalytic activity

Many aeroallergens, such as HDM and pollen, contain proteases[26]. Their protease activity is essential for their allergenicity[27–29]. Therefore, we wanted to test whether the catalytic activity

of SplB is necessary to induce AAI. We generated a catalytically inactive SplB mutant that contains an amino acid switch (S193A) in its catalytic triad. The inactivation of protease activity was confirmed in a substrate assay (Fig. S5A). In this model, ovalbumin (OVA) was used as a control antigen to determine whether the allergic immune response in our model was specific to SplB or induced by the route of application. While active SplB WT induced the expected marked influx of eosinophils into the BAL and the lung tissue (Fig. 3A, C), OVA and the inactive SplB mutant failed to do so. We also observed neutrophils in the BAL of animals that were treated with active SplB but not with OVA or the SplB mutant (Fig. 3B), however, their numbers were very small (mean 2.8 x 10^2 cells per mL BAL) compared to those of the eosinophils (mean 2.1 x 10^5 cells per mL BAL). In the lungs, the numbers of neutrophils did not differ (Fig. 3D), but active SplB induced an influx of DCs (Fig. 3E). To investigate the systemic immune response to i.t. application of SplB, we next analyzed the eosinophil population in the spleen. We found a mild but significant eosinophilia in the spleens of mice sensitized with the active SplB (Fig. 3F), suggesting that SplB-induced AAI leads to systemic immune alterations. Next, we measured type 2 cytokines in the airways. Only active SplB induced IL-4, IL-5, and IL-13 in the BAL (Fig. 3G-I). Likewise, the concentration of the macrophage-derived chemokine (CCL22), a key mediator of T cell recruitment, increased upon i.t. exposure to active SplB but remained low in mice treated with the SplB mutant or with OVA (Fig. 3J).

To assess whether the proteolytic activity of SplB affects the humoral immune response, we measured total and antigen-specific IgE as well as SplB-specific IgG in the serum. The proteolytic activity of SplB was necessary for the production of IgE (Fig. 3K, L). Interestingly, exposure to the enzymatically inactive SplB mutant still provoked a prominent antigen-specific IgG response, that was however lower than that induced by active SplB (Fig. 3M). This shows that the SplB mutant is immunogenic, but not allergenic. OVA-treated mice did not develop OVA-specific antibodies, neither IgE nor IgG (Fig. S5B, C).

Finally, we assessed epithelial barrier damage by quantifying serum albumin and IL-33 concentrations in the lung. Treatment with active SplB significantly increased the albumin concentrations in the BAL, indicating impairment of the epithelial integrity (Fig. 3N). Similarly, the concentration of IL-33 was increased only in the lungs of mice exposed to active SplB, which suggests damage of the epithelial barrier (Fig 3O). The lung concentrations of thymic stromal lymphopoietin (TSLP), granulocyte-macrophage colony-stimulating factor (GM-CSF), IL-1α and IL-25 were below the detection limit.

Taken together, we demonstrated that only mice sensitized with the enzymatically active SplB developed asthma symptoms and signs of a type 2 immune response, while those exposed to OVA or the inactive SplB mutant did not. This finding indicates that the enzymatic activity of SplB is necessary for the establishment of AAI.

IL-33 is a crucial mediator in SplB-induced AAI

IL-33 is an essential signaling molecule in asthma[30]. To elucidate the role of IL-33 in SplB-induced asthma, we co-administered the IL-33 inhibitor HpARI2 with SplB. In a parallel approach we tested the effect of SplB on IL-33 ko mice. Control mice received PBS. HpARI2 completely abolished the SplB-induced AHR following methacholine challenge (Fig. 4A). In line with this, WT mice challenged with SplB alone showed a marked accumulation of eosinophils in the lung (Fig. 4B, D). Of note, only the SplB-treated IL-33 ko mice displayed a significant difference towards SplB-treated WT mice. Although co-application of the IL-33 inhibitor markedly reduced airway eosinophilia, the reduction was not significant compared to SplB-treated WT mice. The numbers of DCs and $CD4^+$ T cells were not affected in the mice treated with the inhibitor and IL-33 ko mice in a statistically significant way compared to the SplB-treated mice (Fig. 4 C, E, F). Remarkably, the anti-SplB IgE titers increased in the sera of all SplB-treated mice, independent of the IL-33 activity (Fig. 4G). This demonstrates that although IL-33 is crucial for recruiting eosinophils to the site of inflammation, it is not required for the immunoglobulin class switch of the specific antibody-producing plasma cells.

Numerous allergens cleave the alarmin IL-33, which increases its biological activity and leads to the activation of innate immune cells and Th2 cells[24]. Since both the catalytic activity of SplB and IL-33 are essential for the induction of AAI, we tested whether the SplB targets IL-33. We incubated full-length human (hIL-33) or murine IL-33 (mIL-33) with SplB at 37 °C for 2.5 and 24 hours and visualized the cleavage patterns with Coomassie staining and Western blotting. SplB cleaved human, but not murine IL-33 as lower molecular weight bands (< 25 kDa) appeared only in samples of hIL-33 (Fig. 5).

PAR2 is dispensable for the development of SplB-induced AAI

PAR2 activation by protease allergens promotes Th2-mediated inflammation in the lung and increased PAR2 expression is associated with increased asthma severity[31]. We therefore investigated the role of PAR2 in SplB-induced murine AAI by treating PAR2 ko mice with SplB and applying a PAR2-blocking antibody together with SplB in WT mice. PAR2-deficient mice exposed to SplB displayed the same number of inflammatory cells in their BAL and lungs as their WT counterparts (Fig. 6A-C). Likewise, PAR2-competent and -deficient mice had similar titers of anti-SplB IgE in their sera (Fig. 6D). Similarly, blocking of PAR2 with a monoclonal antibody failed to protect mice from AAI (Fig. S6). We conclude that PAR2 is not required for the development of SplB-induced AAI.

Discussion

In this study, we show that the protease SplB, which is secreted by *S. aureus*, is a potent allergen that induces type 2 airway inflammation in mice. Four intratracheal applications of the recombinant enzyme were sufficient for this without the need for adjuvants or prior intraperitoneal priming. The AAI phenotype induced by SplB was characterized by increased AHR, influx of inflammatory cells into the lung, and a prominent adaptive immune response with production of SplB-specific IgE. The AAI phenotype depended on the adaptive immune system because Rag2 ko mice, which lack T cells and B cells, did not develop asthma.

In WT mice, the IgE response was bi-phasic: high titers of total and SplB-specific IgE developed by day 14 and declined by day 24. Upon contact with their antigen, naïve B cells first develop into plasmablasts. The plasmablasts dominate the early antibody response, but most have a short lifespan and only a small fraction further differentiates into long-lived plasma cells[32,33]. We therefore suspect that the high IgE titers on day 14 are mainly attributable to plasmablasts, whereas the lower titers observed at later stages reflect the activity of plasma cells.

In our model, the allergenic potential of SplB was strictly dependent on its proteolytic activity, as the catalytically inactive SplB mutant failed to elicit AAI. Remarkably, in contrast to OVA, the SplB mutant still induced a specific IgG response. The absence of an immune response to OVA could be attributed to its eukaryotic origin, therefore it shares structural similarities with host proteins[34,35]. In contrast, SplB may contain structural motifs conserved in bacteria that are

recognized by cell surface receptors, thereby triggering an adaptive immune response without promoting type 2 polarization[36].

Since catalytically active SplB increased IL-33 concentrations in the lung, we speculated that SplB induces AAI by activating the IL-33 signaling pathway. To elucidate the role of IL-33 in our model, we exposed IL-33-deficient mice to SplB. In a second approach we blocked IL-33 signaling in WT mice with HpARI2, a potent anti-IL-33 agent originally derived from helminths[37]. In the absence of IL-33 signaling, SplB did not induce eosinophilic airway inflammation. In contrast, IL-33 was not required for the induction of a SplB-directed adaptive immune response of type 2 with immunoglobulin class switch to IgE. We conclude that other mediators than IL-33 must have induced the sensitization to SplB, which involves the maturation of naïve DCs into cDC2s to drive the polarization of Th2 cells[38,39]. A candidate for this is TSLP, an alarmin known to be essential for cDC2 maturation[40]. The concentrations of TSLP, however, remained below the limit of detection. Our readout 72 h after the last SplB challenge may have been too late, as alarmins are quickly released upon epithelial stimulation[41]. Next, T follicular helper (Tfh) cells are critical for B cell activation and the immunoglobulin class switch in the germinal centers[42]. These Tfh cells, however, do not express the IL-33 receptor ST2 and are thus independent of IL-33 signaling[43]. In contrast, mast cells express ST2 at high density, and IL-33 lowers their degranulation threshold[44,45]. Mast cells release IL-5 upon degranulation, which is critical for eosinophil recruitment[46]. A lack of mast-cell derived IL-5 could explain the absence of eosinophils in mice without active IL-33. Although both IL-33 and catalytic activity of SplB were essential, murine IL-33 could not be verified as a direct target of SplB.

We reasoned that SplB causes murine asthma by cleaving another substrate, possibly the membrane-bound protease sensor PAR2, which is targeted by several known protease allergens[22,47]. However, SplB induced AAI independently of PAR2 activation. This is not unprecedented as other studies have shown that HDM can induce AAI independent of PAR2[48,49].

Epithelial barriers are the first line of defense against environmental threats like pathogens and allergens. *S. aureus* needs to overcome host barriers to persist and cause infections. It has been shown that Spls play a role in bacterial spread in a rabbit pneumonia model, suggesting that the bacterial proteases damage barriers[50]. In line, SplB is able to disrupt endothelial barriers and cause vascular leakage[51]. In this study we have shown that SplB also disrupts the airway

epithelial barrier in AAI and causes influx of serum albumin into the airways. We speculate that SplB induces barrier disruption through direct or indirect interference with tight junctions, analogous to other protease allergens[19,52,53]. However, the underlying mechanism remains to be elucidated in future studies.

Our study advances our understanding of the role of *S. aureus* colonization in the pathogenesis of asthma. This is currently a matter of debate and two mutually non-exclusive hypotheses have been proposed: (1) Asthma and the associated type 2 immune response facilitate *S. aureus* colonization and (2) *S. aureus* colonization creates a type 2 microenvironment promoting allergic sensitization towards harmless antigens[8]. Based on our results we propose a third hypothesis to complement these two scenarios: (3) *S. aureus* secretes allergens that can induce asthma development and trigger asthma attacks. We have identified SplB as a potent allergen that causes severe eosinophilic lung inflammation on its own without exogenous adjuvants or systemic priming. SplB elicited the production of allergen-specific IgE in both mice and humans[14,15], and promoted airway hyperresponsiveness in response to methacholine challenge. Other members of the Spl family, namely SplD and SplF, also induce IL-33-dependent AAI in mice[13]. Thus, *S. aureus* may play a more active role in asthma than previously thought. Consequently, *S. aureus* decolonization strategies may hold therapeutic potential for alleviating asthma symptoms and improving the long-term disease outcome in sensitized patients.

Methods

Recombinant protein production

Recombinant SplB and SplB mutant were produced in the *S. aureus* strain RN4220 using the expression vector pTripleTREP[54]. The sequence of SplB was derived from the *S. aureus* strain USA300 FPR3757. An amino acid switch (S193A) was introduced into the catalytic triad of the mutant to achieve catalytic inactivity. Cell-free culture supernatants were collected and the SplB and SplB mutant were isolated via a C-terminal twin-strep-tag. In brief, supernatant was incubated with MagStrep Type 3 XT beads (ThermoFisher Scientific, Waltham, USA; MA5-16779), whereby the tagged proteases bound to the beads. Beads were washed three times with DPBS to remove contaminant proteins. The protease was eluted from the beads by adding 100 mM biotin in DPBS. The elution step was repeated three times and the eluate filtered

through a 0.3 µm filter to remove possible bacterial contaminations. The biotin was removed using 10 kDa centrifugal filter units (Merck Millipore, Billerica, USA). Thereby the buffer was exchanged with DPBS. LPS contamination was checked using the Endosafe Portable Test System (Charles River, Wilmington, USA). The quality of the SplB WT and SplB mutant preparation was assessed by SDS-PAGE, western blot and MS analysis[54]. Recombinant tag-free SplB was expressed in *B. subtilis* as described previously[13]. Recombinant endotoxin-free ovalbumin was purchased (InvivoGen, San Diego, USA; vac-pova). Recombinant HpARI2 was kindly provided by Dr. Henry McSorley (Institute for Cell Signalling and Immunology, University of Dundee, UK).

Mice

Animals were maintained in a 12-hour/12-hour light/dark cycle and had access to water and food *ad libitum*. Animal experiments were approved by the Landesamt für Landwirtschaft, Lebensmittelsicherheit und Fischerei Mecklenburg-Vorpommern (LALLF MV; AZ 7221.3-1-037/20). The following mouse strains were used: C57BL/6J, C57BL/6J-Rag2em3Lutzy/J (RAG2 ko in C57BL/6J background), C57BL/6J IL-33$^{Gt/Gt}$ (IL-33 ko in C57BL/6J background) and B6.Cg-F2rl1tm1Mslb/J (PAR2 ko in C57BL/6J background). Mice were purchased from Janvier (C57BL/6J), JAX (C57BL/6J RAG2 ko; C57BL/6J PAR2 ko) or bread in-house (C57BL/6J IL-33 ko). Mice were ordered as *S. aureus*-free. All mice used in animal experiments were female and 8-12 weeks old when treatment started.

Mouse asthma model and sensitization protocol

C57BL/6J mice were put under anesthesia and treated i.t. with PBS, SplB WT (10, 25 or 50 µg), SplB mutant (25 µg) or OVA (50 µg) on day 0, 7, 14 and 21. Proteins were dissolved in 50 µL DPBS. In some experiments, HpARI2 (10 µg), SAM-11 (10 ng; ThermoFisher Scientific, Waltham, USA; 35-2300) or IgG isotype-antibody (10 ng; ThermoFisher Scientific, Waltham, USA; 02-6200) were i.t. co-applied with SplB. On day 0, 7 and 14, approximately 100 µL blood was taken via the retroorbital plexus prior to challenge. 72 hours after the fourth treatment, mice were anesthetized and the AHR was measured. Mice were sacrificed with an overdose of

isoflurane afterwards. Bronchoalveolar lavage (BAL), blood, mediastinal lymph nodes (mLN), lungs and spleen were recovered.

Airway hyperreactivity test

AHR was measured by forced oscillation technic using a FlexiVent system (Scireq, Montreal, Canada) 72 h after the last challenge. After putting the animal under deep anesthesia (75 mg/kg ketamine + 5 mg/kg xylazine), the trachea was exposed by surgical incision of the throat area. A small horizontal incision was made in the upper part of the trachea, a canula was inserted and fixated. Afterwards, the mouse was connected to the FlexiVent and mechanically ventilated at a pressure of 3 cm H2O with 150 breaths per minute. Spontaneous breathing was prevented by i.p. injection with 2,5 mg/kg bodyweight rocuronium bromide (Inresa Arzneimittel GmbH, Freiburg im Breisgau, Germany). Acetyl-β-Methyl-Choline (methacholine) (Sigma-Aldrich, München, Germany) was aerosolized in a nebulizer and delivered with increasing doses (0, 5, 10, 20, 50, 100 mg/mL) through inhalation. Airway resistance was measured throughout the next two minutes after application.

Organ processing

Blood was collected via the retroorbital plexus (day 0, 7 and 14) or via aortic puncture (day 24) and centrifuged (16,000× g, 4 °C, 10 min). The serum was collected and stored at -80 °C. A broncho-alveolar lavage (BAL) was performed to characterize cell populations and cytokines in the lung lumen. 1 mL of PBS was injected into the airways and slowly retracted with a syringe. The procedure was performed three times per mouse. BAL was centrifuged (300× g, 10 min, 4 °C), cell-free supernatant was taken off and the volume was recorded. Supernatants were stored at -80 °C. Cells were resuspended in 500 µL PBS and proceeded to flow cytometry analysis. Lungs were perfused with 5 mL PBS through the right ventricle. The upper part of the left lung was fixed in 4% formalin for histology. The lower part of the left lung lobe and the postcaval lobe were snap-frozen with liquid nitrogen. Superior, middle and inferior lobe were kept in RPMI at 4 °C. These lobes were digested with 200 µg liberase (Sigma-Aldrich, München Germany; 05401020001) and 800 µg of DNase (Sigma-Aldrich, München, Germany; 10104159001) in 2.5 mL RPMI medium. Lungs were minced using the GentleMACS (Miltenyi

Biotec, Bergisch Gladbach, Germany). Afterwards, lungs were incubated in a water bath (37 °C, 30 min, 100 rpm). To get a single cell suspension, lungs were homogenized in the GentleMACS. The suspension was then filtered through a 70 µm cell strainer to remove remaining fat tissue and collagen fibers. Cells were washed and centrifuged (300× g, 10 min, 4 °C). Afterwards, the cells were resuspended in erythrocyte lysis buffer. Lysis was stopped and cells were again centrifuged (300× g, 10 min, 4 °C), resuspended in 1 mL RPMI medium and proceeded to flow cytometry analysis. Spleen was removed, a small part was snap-frozen with liquid nitrogen, another part was kept in RPMI at 4 °C for single cell isolation. Spleens were meshed through a 70 µm cell strainer to get a single cell suspension. Cells were washed with RPMI medium and centrifuged (300× g, 10 min, 4 °C). Afterwards, the cells were resuspended in erythrocyte lysis buffer. Lysis was stopped and cells were again centrifuged (300× g, 10 min, 4 °C), resuspended in 2 mL RPMI medium and proceeded to flow cytometry analysis.

Flow cytometry

First, cells from BAL, lung and spleen were counted on the BD LSR II flow cytometer (BD, Franklin Lakes, USA) using TruCount beads (BD, Franklin Lakes, USA). For flow cytometry staining, 1 million cells were incubated with Fc block solution (Miltenyi Biotech, Bergisch Gladbach, Germany) and stained with fixable live/dead stain (BioLegend, San Diego, US). BAL and spleen were stained with one, the lung with two antibody panels, which are described in detail below. Unless noted, all antibodies were purchased from Miltenyi (Miltenyi Biotech, Bergisch Gladbach, Germany). Data were acquired using a BD LSR II flow cytometer and analyzed using the FlowJo software (V10.10.0). To quantify BAL cells, the total number of cells in the BAL was determined and calculated to the number of cells per mL of BAL. The recorded volume of total lavage collected was used for this calculation. The percentage of each population in the number of cells per mL was then determined and used to calculate the total number of cells per mL of lavage. To analyze the lung cell populations, the percentage of cell types as part of the live cells was first calculated. This percentage was then applied to the total number of cells to get the total number of cells in three lobes. To analyze the spleen cell populations, the percentages of cells were compared.

BAL panel:

BAL was stained to quantify eosinophils, neutrophils and $CD4^+$ T cellsin the lung lumen. The following antibodies were used: anti-mouse CD4-VioBlue (130-118-696), CD11c-allophycocyanin (APC) (130-110-839), Ly6-G-fluorescein isothiocyanate (FITC) (130-120-820) and Siglec-F-phycoerythrin (PE)-Vio770 (130-112-334).

Lung panel 1:

The panel was used to quantify eosinophils, neutrophils and DCs in the lung tissue. The following antibodies were used: anti-mouse Ly6-G-FITC (130-120-820), MHC Class II-Viogreen (130-112-395), CD103-APC (130-111-686), CD11b-PE-Vio770 (130-113-808), CD64-PE (130-118-684), Siglec-F-PE-Vio615 (130-112-330) and CD11c-VioBlue (130-110-843). The following antibodies were used for dump channel: anti-mouse CD19-APC-Vio770 (130-112-038), CD3-APC-Vio770 (130-119-793) and CD49b-APC-Vio770 (130-116-435).

Lung panel 2:

The panel was used to quantify T cells in the lung tissue. The following antibodies were used: anti-mouse CD3-peridinin-chlorophyll-protein complex (PerCP)-Vio700 (130-120-826), MHC Class II-Viogreen (130-112-395), CD4-Brilliant Violet 605 (BioLegend, San Diego, USA; 100548), CD11b-PE-Vio770 (130-113-808), CD44-VioBright FITC (130-120287), NK1.1-PE (130-120-506), CD11c-VioBlue (130-110-843) and CD62L-APC (130-112-837).

Spleen panel:

Spleen was stained to quantify eosinophils, T and B cells in the periphery to determine systemic inflammation. The following antibodies were used: anti-mouse Siglec-F-PE-Vio770 (130-112-334), CD11c-APC (130-110-839), CD3-PerCP-Vio700 (130-120-826), CD4-VioBlue (130-118-696), CD8-PE (BioLegend, San Diego, USA; 100708), CD45R-Brilliant Violet 510 (BioLegend, San Diego, USA; 103248) and CD19-Brilliant Violet 650 (BioLegend, San Diego, USA; 115541).

Lung homogenization

Lung tissue was homogenized for protein analysis. First, a 2 mL homogenizer tube was filled with 250 µL RIPA lysis buffer (Sigma-Aldrich, München, Germany) supplemented with protease inhibitors and six 2.8 mm and 200 µL of 1.5 mm zirconium oxide beads (Bertin Technologies, Montigny-le-Bretonneux, France). Tissue was transferred into the tube and homogenized in a Precellys 24 (6000 rpm; 2x20 s) (Bertin Technologies, Montigny-le-Bretonneux, France). The supernatant was collected and transferred to a 1.5 mL tube. Protein concentration was determined by BCA assay (ThermoFisher Scientific, Waltham, USA; 23225).

ELISA

SplB- and OVA-specific IgE and IgG was measured with ELISA as described previously[13]. In brief, plates were coated with 2 µg/mL tag-free SplB or OVA. Tag-free SplB expressed in *B. subtilis* was used for coating because the twin-strep tag interfered with the ELISA. For IgE ELISA, serum was diluted 1:10, whereas for IgG ELISA it was diluted 1:10,000. After blocking, 50 µL sample was applied and the plate was incubated. After washing, the plate was incubated with 50 µL of 1 µg/mL detection antibody (rat anti-mouse IgE (ThermoFisher Scientific, Waltham, USA; MA5-16779) or rat anti-mouse IgG (Jackson ImmunoResearch, West Baltimore Pike, USA; 115-065-164)). Following another washing step, the plate was incubated with 50 µL 0,33 µg/mL horseradish peroxidase (HRP) (Dianova, Hamburg, Germany; 016-030-084). After final washing, TMB substrate (BD Biosciences, Heidelberg, Germany) was added and the reaction was stopped after 20 min of incubation using 2N H_2SO_4. Absorbance was measured at 450 nm on a TECAN Infinite M200 plate reader (Tecan Group Ltd., Maennedorf, Switzerland). Total IgE concentration in the serum was measured by ELISA according to the manufacturer's instructions (BioLegend, San Diego, USA; 432401). Total serum albumin concentration in the BAL was measured by ELISA according to the manufacturer's instructions (Antibodies.com, Cambridge, UK; A4028). Concentration of cytokines (IL-33, TSLP, GM-CSF, IL-1α, IL-25) was quantified using kits from both ThermoFisher Scientific (Waltham, USA; IL-33, 88-7333-88) and BioLegend (San Diego, USA; TSLP, 434104; GM-CSF, 432204; IL-1α, 433401; IL-25, 447104) according to the manufacturer's instructions. Cytokine concentration was measured in mouse lung homogenate containing 50 µg of total protein.

Cytometric Bead Array (CBA) measurements

A CBA is a multiplex assay that uses antibody-coated fluorescent beads in flow cytometry to simultaneously measure multiple cytokines in a single sample. Two CBA kits were used to quantify cytokines and chemokines in the BAL (BioLegend, San Diego, USA; 741043 and 740007). Analysis was performed using the Qognit website (version: 2024-06-15).

Substrate Assay

A substrate-specific cleavage assay was performed to confirm the catalytic activity of SplB WT and the inactivity of the SplB mutant. For this purpose, the synthetic peptide Ac-VEID-AMC (PeptaNova GmbH, Sandhausen, Germany), which contains a validated SplB cleavage site[55], was used. The peptide is covalently linked to 7-amino-4-methylcoumarin (AMC), which is released as a fluorescent product upon cleavage. Fluorescence intensity was quantified over time using a TECAN Infinite M200 plate reader (Tecan Group Ltd., Maennedorf, Switzerland). PBS and heat-inactivated SplB WT (95 °C, 30 min) served as negative controls.

Cleavage assay

To test whether SplB is capable of cleaving human and murine IL-33, SplB WT was incubated with hIL33 (OriGene Technologies, Inc., Rockville, US; TP760633) and mIL33 (OriGene Technologies, Inc., Rockville, US; TP607659). Equimolar concentrations of SplB and IL-33 were used and two different incubation times (2.5 h and 24 h) at 37 °C were tested. Cleavage was analyzed by Coomassie staining and western blotting.

Western Blotting (WB)

0.5 µg of digested hIL-33 or mIL-33 were loaded on a 10% Tris/HCl gel and separated by SDS-PAGE. Afterwards, proteins were blotted onto a PVDF membrane. Goat anti-human IL-33

(R&D Systems, Minneapolis, USA; AF3625; dilution 1:10,000) or goat anti-mouse IL-33 (R&D Systems, Minneapolis, USA; AF3626; dilution 1:10,000) was used in combination with HRP-conjugated donkey anti-goat IgG (R&D Systems, Minneapolis, US; HAF109; dilution 1:10,000) for target detection. Bands were visualized with the Maximum Sensitivity Substrate (ThermoFisher Scientific, Waltham, USA).

Statistics

All datasets were tested for normality using the Shapiro–Wilk test. Ordinary one-way ANOVA was used if all datasets were normally distributed, otherwise the Kruskal–Wallis test was applied. AHR measurements were analyzed using a two-way ANOVA. A p value < 0.05 was considered significant. Statistical analyses were performed with GraphPad Prism v8.0.1. Data are shown as median with interquartile range if more than one group consisted of ≤ 4 animals, because the median and interquartile range are more robust to outliers, and as mean ± SD otherwise.

Figure legends

Figure 1

SplB induces allergic airway inflammation in mice. **A**, Mouse model of chronic allergic airway inflammation. Mice received 4 intratracheal (i.t.) applications every 7 days of either PBS or differing doses of SplB and were killed 72 hours after the last application. **B**, Airway resistance in response to increased doses of methacholine administered 72 hours after the last i.t. challenge was measured using a forced oscillation technique. **C-F**, Total cell count (C), inflammatory eosinophils (D), neutrophils (E) and $CD4^+$ T cells (F) in bronchoalveolar lavage (BAL) quantified by flow cytometry staining. **G-M**, Total cell count (G), inflammatory eosinophils (H), neutrophils (I), $CD4^+$ T cells (J), ratio of naïve over effector T cells (K), Dendritic cells (DCs) (L) and DC subsets (M) in lung tissue quantified by flow cytometry staining. **N**, SplB-specific IgE over the course of the experiment measured by ELISA. n = 3-7. Results are presented as median with interquartile range. *$p < .05$, **$p < .01$ and ***$p < .005$. Significance

was determined using a one-way ANOVA. AHR measurements were analyzed using a two-way ANOVA.

Figure 2

SplB-induced AAI depends on an intact adaptive immune system. WT or Rag2 ko C57BL/6 J mice were treated with SplB, PBS-treated Rag2 ko mice served as control. **A**, Number of inflammatory eosinophils in the BAL measured by flow cytometry. **B** and **C**, Number of inflammatory eosinophils (B) and DCs (C) in the lung measured by flow cytometry. n = 3-6. Results are presented as mean with SD. *p < .05 and ***p < .005. Significance was determined using a Kruskal Wallis test.

Figure 3

Catalytic activity of SplB is essential to cause AAI. WT C57BL/6 J mice were treated with active SplB or a catalytically inactive SplB mutant, OVA-treated mice served as control. **A** and **B**, Number of inflammatory eosinophils (A) and neutrophils (B) in the BAL measured by flow cytometry. **C-E**, Number of inflammatory eosinophils (C), neutrophils (D) and DCs (E) in the lung measured by flow cytometry. **F**, Number of eosinophils in the spleen measured by flow cytometry. **G-J**, Concentration of IL-4 (G), IL-5 (H), IL-13 (I) and CCL22 (J) the BAL measured by CBA. **K-M**, Total IgE (K), SplB-specific IgE (L) and SplB-specific IgG on day 14 and 24 of the experiment measured by ELISA. **N**, serum albumin concentration in the BAL measured by ELISA. **O**, IL-33 concentration in 50 µg of lung protein measured by ELISA. n = 5-9. Results are presented as mean with SD. *p < .05, **p < .01 and ***p < .005. Significance was determined using a Kruskal Wallis test, except for N and O, where significance was determined using a one-way ANOVA.

Figure 4

SplB induced AAI is IL-33-dependent. WT C57BL/6 J mice were treated with SplB or SplB + HpARI2, an IL-33 inhibitor, PBS-treated mice served as control. Additionally, C57BL/6J IL-33 ko mice were treated with either PBS or SplB. **A**, Airway resistance in response to increased doses of methacholine administered 72 hours after the last i.t. challenge was measured using a forced oscillation technique. **B** and **C**, Number of inflammatory eosinophils (B) and $CD4^+$ T cells(C) in the BAL measured by flow cytometry. **D-F**, Number of inflammatory eosinophils (D), $CD4^+$ T cells(E) and DCs (F) in the lung measured by flow cytometry. **G**, SplB-specific

IgE on day 14 and 24 of the experiment measured by ELISA. n = 11-12. Results are presented as mean with SD. *p < .05, **p < .01 and ***p < .005. Significance was determined using a Kruskal Wallis test. AHR measurements were analyzed using a two-way ANOVA.

Figure 5

SplB cleaves full-length hIL-33, but not mIL-33. **A** and **B**, Cleavage of full-length hIL-33. Equimolar concentrations of SplB and hIL-33 were incubated for 2.5 or 24h. Proteins were visualized by Coomassie staining (A) and western blot (B). hIL-33 without prior SplB incubation served as control. Both lanes indicated with an arrow represent SplB. **C** and **D**, Incubation of full-length mIL-33 with SplB. Equimolar concentrations of SplB and mIL-33 were incubated for 2.5 or 24h. Proteins were visualized by Coomassie staining (C) and western blot (D). mIL-33 without prior SplB incubation served as control. One of three similar experiments is shown.

Figure 6

SplB-induced AAI is independent of PAR2 activation. WT or PAR2 ko C57BL/6 J mice were treated with SplB, PBS-treated PAR2 ko mice served as control. **A**, Number of inflammatory eosinophils in the BAL measured by flow cytometry. **B** and **C**, Number of inflammatory eosinophils (B) and DCs (C) in the lung measured by flow cytometry. **D**, SplB-specific IgE over the course of the experiment measured by ELISA. n = 4-8. Results are presented as mean with SD. **p < .01. Significance was determined using a Kruskal Wallis test.

Figure S1

Gating strategy for the BAL. BAL was collected and centrifuged, the supernatant was taken off and the cells were stained for flow cytometry analysis. **A-C** Gating of single cells, exclusion of debris and duplets. **D**, Gating of living cells. **E**, Distinguishing inflammatory eosinophils (SiglecF^{+}; CD11c^{-}) and alveolar macrophages (SiglecF^{+}; CD11^{+}) from SiglecF^{-} cells. **F**, The SiglecF^{-} cells are further distinguished in neutrophils (SiglecF^{-}; Ly6G^{+}) and CD4^{+} T cells (SiglecF^{-}, CD4^{+}).

Figure S2

Gating strategy for the first lung panel to distinguish DC subpopulations. Three lobes of the left lung (superior, middle and inferior lobe) were digested and stained for flow cytometry analysis. **A-C**, Gating of single cells, exclusion of debris and duplets. **D**, Gating of living cells. **E**, Distinguishing inflammatory eosinophils (SiglecF$^+$; CD11c$^-$), resident eosinophils (SiglecF$^+$ low; CD11c), alveolar macrophages (SiglecF$^+$; CD11$^+$) from SiglecF$^-$ cells. **F**, The SiglecF$^-$ cells are further distinguished in dendritic cells (SiglecF$^-$; MHCII$^+$; CD11c$^+$) and MHCII$^-$ cells. **G**, MHCII$^-$ cells were separated into Ly6G$^-$ cells and neutrophils (Ly6G$^+$). **H-I**, DCs subpopulations were further distinguished into type 1 cDCs (SiglecF$^-$; MHCII$^+$; CD11c$^+$, CD103$^+$), type 2 cDCs (SiglecF$^-$; MHCII$^+$; CD11c$^+$, CD103$^-$, CD64$^-$) and moDCs (SiglecF$^-$; MHCII$^+$; CD11c$^+$, CD103$^-$, CD64$^+$).

Figure S3

Gating strategy for the second lung panel to distinguish T cell subpopulations. Three lobes of the left lung (superior, middle and inferior lobe) were digested and stained for flow cytometry analysis. **A-C**, Gating of single cells, exclusion of debris and duplets. **D**, Gating of living cells. **E**, CD3$^-$ cells were separated into NK1.1$^-$ cells and NK cells (CD3$^-$; NK1.1$^+$). **F**, CD4$^-$ T cells (CD3$^+$, CD4$^-$), CD4$^+$ T cells (CD3$^+$, CD4$^+$) were distinguished from CD3$^-$ cells. **G**, CD4$^-$ T cell subpopulations were distinguished into naïve T cells (CD3$^+$, CD4$^-$, CD62L$^+$, CD44$^-$), effector T cells (CD3$^+$, CD4$^+$, CD62L$^-$, CD44$^+$) and memory T cells (CD3$^+$, CD4$^+$, CD62L$^+$, CD44$^+$). **H**, CD4$^+$ T cell subpopulations were distinguished into naïve T cells (CD3$^+$, CD4$^+$, CD62L$^+$, CD44$^-$) and effector T cells (CD3$^+$, CD4$^+$, CD62L$^-$, CD44$^+$).

Figure S4

Gating strategy for the spleen panel. One part of the spleen was separated into single cells and stained for flow cytometry analysis. **A** and **B**, Gating of single cells, exclusion of debris and duplets. **C**, Distinguishing inflammatory eosinophils (SiglecF$^+$; CD11c$^-$) from SiglecF$^-$ cells. **D**, CD3$^+$ cells were distinguished from CD3$^-$ cells. **E**, B-cells (CD3$^-$; CD19$^+$; B220$^+$) were distinguished. **F**, Distinguishing Th cells (CD3$^-$; CD4$^+$, CD8$^-$) from cytotoxic T cells (CD3$^-$; CD4$^-$, CD8$^+$).

Figure S5

Assessment of SplB catalytic activity and OVA-specific antibody responses. **A**, Catalytic inactivity of SplB mutant was assessed using the synthetic peptide substrate Ac-VEID-MCA.

After substrate addition, fluorescence was quantified over 60 min. PBS and heat-inactivated SplB served as negative controls. One out of three similar experiments is depicted. **B** and **C**, OVA-specific IgE (B) and OVA-specific IgG (C) on day 24 of the experiment measured by ELISA, PBS-treated mice served as control. n = 2-4. Results are presented as median with interquartile range.

Figure S6

SplB-induced AAI is independent of PAR2 activation. WT C57BL/6 J mice were treated with SplB or SplB + SAM-11, a PAR2-inhibiting antibody, PAR2 ko mice treated with SplB + IgG2 served as isotype control. **A**, Number of inflammatory eosinophils in the BAL measured by flow cytometry. **B** and **C**, Number of inflammatory eosinophils (B) and DCs (C) in the lung measured by flow cytometry. **D**, SplB-specific IgE over the course of the experiment measured by ELISA. n = 5. Results are presented as mean with SD.

Conflicts of interests

The authors declare that they have no relevant conflicts of interest.

References

1. The Global Asthma Report 2022. *Int. J. Tuberc. Lung Dis.* **26**, 1–104 (2022).
2. Kuruvilla, M. E., Lee, F. E.-H. & Lee, G. B. Understanding Asthma Phenotypes, Endotypes, and Mechanisms of Disease. *Clin. Rev. Allergy Immunol.* **56**, 219–233 (2019).
3. Komlósi, Z. I. *et al.* Cellular and molecular mechanisms of allergic asthma. *Mol. Aspects Med.* **85**, 100995 (2022).
4. Armann, J. & Von Mutius, E. Do bacteria have a role in asthma development? *Eur. Respir. J.* **36**, 469–471 (2010).
5. Laux, C., Peschel, A. & Krismer, B. *Staphylococcus aureus* Colonization of the Human Nose and Interaction with Other Microbiome Members. *Microbiol. Spectr.* **7**, 7.2.34 (2019).

6. Kim, Y.-C. *et al. Staphylococcus aureus* Nasal Colonization and Asthma in Adults: Systematic Review and Meta-Analysis. *J. Allergy Clin. Immunol. Pract.* **7**, 606-615.e9 (2019).

7. Davis, M. F., Peng, R. D., McCormack, M. C. & Matsui, E. C. *Staphylococcus aureus* colonization is associated with wheeze and asthma among US children and young adults. *J. Allergy Clin. Immunol.* **135**, 811-813.e5 (2015).

8. Jorde, I., Schreiber, J. & Stegemann-Koniszewski, S. The Role of *Staphylococcus aureus* and Its Toxins in the Pathogenesis of Allergic Asthma. *Int. J. Mol. Sci.* **24**, 654 (2022).

9. Popowicz, G. M. *et al.* Functional and structural characterization of Spl proteases from *Staphylococcus aureus*. *J. Mol. Biol.* **358**, 270–279 (2006).

10. Baba, T., Bae, T., Schneewind, O., Takeuchi, F. & Hiramatsu, K. Genome Sequence of *Staphylococcus aureus* Strain Newman and Comparative Analysis of Staphylococcal Genomes: Polymorphism and Evolution of Two Major Pathogenicity Islands. *J. Bacteriol.* **190**, 300–310 (2008).

11. Reed, S. B. *et al.* Molecular Characterization of a Novel *Staphylococcus aureus* Serine Protease Operon. *Infect. Immun.* **69**, 1521–1527 (2001).

12. Gimza, B. D. *et al.* Unraveling the Impact of Secreted Proteases on Hypervirulence in *Staphylococcus aureus*. *mBio* **12**, e03288-20 (2021).

13. Teufelberger, A. R. *et al.* The IL-33/ST2 axis is crucial in type 2 airway responses induced by *Staphylococcus aureus*-derived serine protease-like protein D. *J. Allergy Clin. Immunol.* **141**, 549-559.e7 (2018).

14. Stentzel, S. *et al.* Staphylococcal serine protease–like proteins are pacemakers of allergic airway reactions to *Staphylococcus aureus*. *J. Allergy Clin. Immunol.* **139**, 492-500.e8 (2017).

15. Nordengrün, M. *et al.* Allergic Reactions to Serine Protease-Like Proteins of *Staphylococcus aureus*. *Front. Immunol.* **12**, 651060 (2021).

16. Thomas, W. R., Hales, B. J. & Smith, W.-A. House dust mite allergens in asthma and allergy. *Trends Mol. Med.* **16**, 321–328 (2010).

17. Taylor, P. E., Jacobson, K. W., House, J. M. & Glovsky, M. M. Links between pollen, atopy and the asthma epidemic. *Int. Arch. Allergy Immunol.* **144**, 162–170 (2007).

18. Arruda, L. K. *et al.* Cockroach allergens and asthma. *J. Allergy Clin. Immunol.* **107**, 419–428 (2001).

19. Wan, H. *et al.* Der p 1 facilitates transepithelial allergen delivery by disruption of tight junctions. *J. Clin. Invest.* **104**, 123–133 (1999).

20. Chen, J.-C. *et al.* The Protease Allergen Pen c 13 Induces Allergic Airway Inflammation and Changes in Epithelial Barrier Integrity and Function in a Murine Model. *J. Biol. Chem.* **286**, 26667–26679 (2011).

21. Kale, S. L., Agrawal, K., Gaur, S. N. & Arora, N. Cockroach protease allergen induces allergic airway inflammation via epithelial cell activation. *Sci. Rep.* **7**, 42341 (2017).

22. Li, B. *et al.* Dust mite-derived Der f 3 activates a pro-inflammatory program in airway epithelial cells via PAR-1 and PAR-2. *Mol. Immunol.* **109**, 1–11 (2019).

23. Sun, G., Stacey, M. A., Schmidt, M., Mori, L. & Mattoli, S. Interaction of mite allergens Der p3 and Der p9 with protease-activated receptor-2 expressed by lung epithelial cells. *J. Immunol. Baltim. Md 1950* **167**, 1014–1021 (2001).

24. Cayrol, C. *et al.* Environmental allergens induce allergic inflammation through proteolytic maturation of IL-33. *Nat. Immunol.* **19**, 375–385 (2018).

25. Hiraishi, Y. *et al.* IL-33, IL-25 and TSLP contribute to development of fungal-associated protease-induced innate-type airway inflammation. *Sci. Rep.* **8**, 18052 (2018).

26. Soh, W. T. *et al.* Protease allergens as initiators–regulators of allergic inflammation. *Allergy* **78**, 1148–1168 (2023).

27. Snelgrove, R. J. *et al.* Alternaria-derived serine protease activity drives IL-33–mediated asthma exacerbations. *J. Allergy Clin. Immunol.* **134**, 583-592.e6 (2014).

28. Gough, L., Schulz, O., Sewell, H. F. & Shakib, F. The Cysteine Protease Activity of the Major Dust Mite Allergen Der P 1 Selectively Enhances the Immunoglobulin E Antibody Response. *J. Exp. Med.* **190**, 1897–1902 (1999).

29. Gough, L., Campbell, E., Bayley, D., Van Heeke, G. & Shakib, F. Proteolytic activity of the house dust mite allergen Der p 1 enhances allergenicity in a mouse inhalation model. *Clin. Exp. Allergy J. Br. Soc. Allergy Clin. Immunol.* **33**, 1159–1163 (2003).

30. Cayrol, C. & Girard, J.-P. Interleukin-33 (IL-33): A critical review of its biology and the mechanisms involved in its release as a potent extracellular cytokine. *Cytokine* **156**, 155891 (2022).

31. Gandhi, V. D., Shrestha Palikhe, N. & Vliagoftis, H. Protease-activated receptor-2: Role in asthma pathogenesis and utility as a biomarker of disease severity. *Front. Med.* **9**, 954990 (2022).

32. Nutt, S. L., Hodgkin, P. D., Tarlinton, D. M. & Corcoran, L. M. The generation of antibody-secreting plasma cells. *Nat. Rev. Immunol.* **15**, 160–171 (2015).

33. Tarlinton, D., Radbruch, A., Hiepe, F. & Dörner, T. Plasma cell differentiation and survival. *Curr. Opin. Immunol.* **20**, 162–169 (2008).

34. Benarafa, C. & Remold-O'Donnell, E. The ovalbumin serpins revisited: Perspective from the chicken genome of clade B serpin evolution in vertebrates. *Proc. Natl. Acad. Sci.* **102**, 11367–11372 (2005).

35. De Groot, A. S., Khan, S., Mattei, A. E., Lelias, S. & Martin, W. D. Does human homology reduce the potential immunogenicity of non-antibody scaffolds? *Front. Immunol.* **14**, (2023).

36. Chen, R. *et al.* Pattern recognition receptors: function, regulation and therapeutic potential. *Signal Transduct. Target. Ther.* **10**, 216 (2025).

37. Osbourn, M. *et al.* HpARI Protein Secreted by a Helminth Parasite Suppresses Interleukin-33. *Immunity* **47**, 739-751.e5 (2017).

38. Xu, J. *et al.* The role of DC subgroups in the pathogenesis of asthma. *Front. Immunol.* **15**, 1481989 (2024).

39. Ronchese, F., Webb, G. R., Ochiai, S., Lamiable, O. & Brewerton, M. How type-2 dendritic cells induce Th2 differentiation: Instruction, repression, or fostering T cell-T cell communication? *Allergy* **80**, 395–407 (2025).

40. Smolinska, S., Antolín-Amérigo, D., Popescu, F.-D. & Jutel, M. Thymic Stromal Lymphopoietin (TSLP), Its Isoforms and the Interplay with the Epithelium in Allergy and Asthma. *Int. J. Mol. Sci.* **24**, 12725 (2023).

41. Takai, T. TSLP Expression: Cellular Sources, Triggers, and Regulatory Mechanisms. *Allergol. Int.* **61**, 3–17 (2012).

42. Song, W. & Craft, J. T Follicular Helper Cell Heterogeneity. *Annu. Rev. Immunol.* **42**, 127–152 (2024).

43. Kobayashi, T., Iijima, K., Dent, A. L. & Kita, H. Follicular helper T cells mediate IgE antibody response to airborne allergens. *J. Allergy Clin. Immunol.* **139**, 300-313.e7 (2017).

44. Saluja, R., Khan, M., Church, M. K. & Maurer, M. The role of IL-33 and mast cells in allergy and inflammation. *Clin. Transl. Allergy* **5**, 33 (2015).

45. Taracanova, A. *et al.* Substance P and IL-33 administered together stimulate a marked secretion of IL-1β from human mast cells, inhibited by methoxyluteolin. *Proc. Natl. Acad. Sci.* **115**, (2018).

46. AbuJabal, R., Ramakrishnan, R. K., Bajbouj, K. & Hamid, Q. Role of IL-5 in asthma and airway remodelling. *Clin. Exp. Allergy J. Br. Soc. Allergy Clin. Immunol.* **54**, 538–549 (2024).

47. Page, K., Strunk, V. S. & Hershenson, M. B. Cockroach proteases increase IL-8 expression in human bronchial epithelial cells via activation of protease-activated receptor (PAR)-2 and extracellular-signal-regulated kinase. *J. Allergy Clin. Immunol.* **112**, 1112–1118 (2003).

48. Lee, H. Y. *et al.* Role of the protease-activated receptor-2 (PAR2) in the exacerbation of house dust mite-induced murine allergic lung disease by multi-walled carbon nanotubes. *Part. Fibre Toxicol.* **20**, 32 (2023).

49. Post, S. *et al.* Protease-Activated Receptor-2 Activation Contributes to House Dust Mite-Induced IgE Responses in Mice. *PLoS ONE* **9**, e91206 (2014).

50. Paharik, A. E. *et al.* The Spl Serine Proteases Modulate *Staphylococcus aureus* Protein Production and Virulence in a Rabbit Model of Pneumonia. *mSphere* **1**, e00208-16 (2016).

51. Iqbal, J. *et al.* Monoclonal antibody neutralizes *Staphylococcus aureus* serine protease-like protein B (SplB)-induced pathology. *Infect. Immun.* **93**, e00171-25 (2025).

52. Vinhas, R. *et al.* Pollen proteases compromise the airway epithelial barrier through degradation of transmembrane adhesion proteins and lung bioactive peptides. *Allergy* **66**, 1088–1098 (2011).

53. Grozdanovic, M. M. *et al.* Kiwifruit cysteine protease actinidin compromises the intestinal barrier by disrupting tight junctions. *Biochim. Biophys. Acta BBA - Gen. Subj.* **1860**, 516–526 (2016).

54. Wolfgramm, H. *et al.* pTripleTREP – A vector for tightly controlled expression and purification of virulence factors in *Staphylococcus aureus*. *Microb. Cell Factories* **24**, 115 (2025).

55. Dubin, G. *et al.* Enzymatic activity of the *Staphylococcus aureus* SplB serine protease is induced by substrates containing the sequence Trp-Glu-Leu-Gln. *J. Mol. Biol.* **379**, 343–356 (2008).

Figure 1

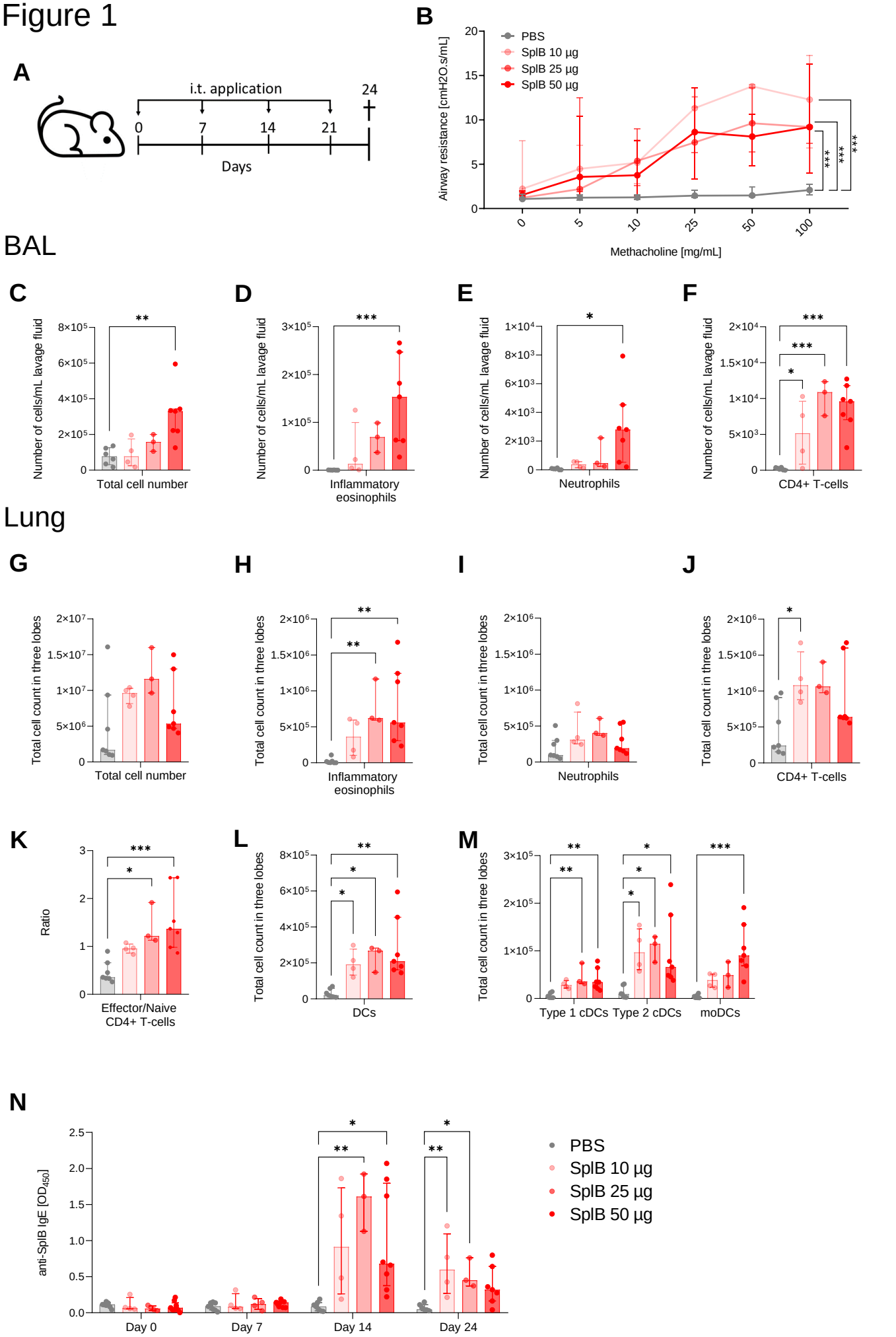
A
i.t. application
0
7
14
21
24
Days
B
PBS
SplB 10 µg
SplB 25 µg
SplB 50 µg
Airway resistance [cmH2O.s/mL]
Methacholine [mg/mL]
BAL
C
Number of cells/mL lavage fluid
Total cell number
D
Inflammatory eosinophils
E
Neutrophils
F
CD4+ T-cells
Lung
G
Total cell count in three lobes
Total cell number
H
Inflammatory eosinophils
I
Neutrophils
J
CD4+ T-cells
K
Ratio
Effector/Naive CD4+ T-cells
L
DCs
M
Type 1 cDCs
Type 2 cDCs
moDCs
N
anti-SplB IgE [OD450]
Day 0
Day 7
Day 14
Day 24
PBS
SplB 10 µg
SplB 25 µg
SplB 50 µg

Figure 2

BAL

Lung

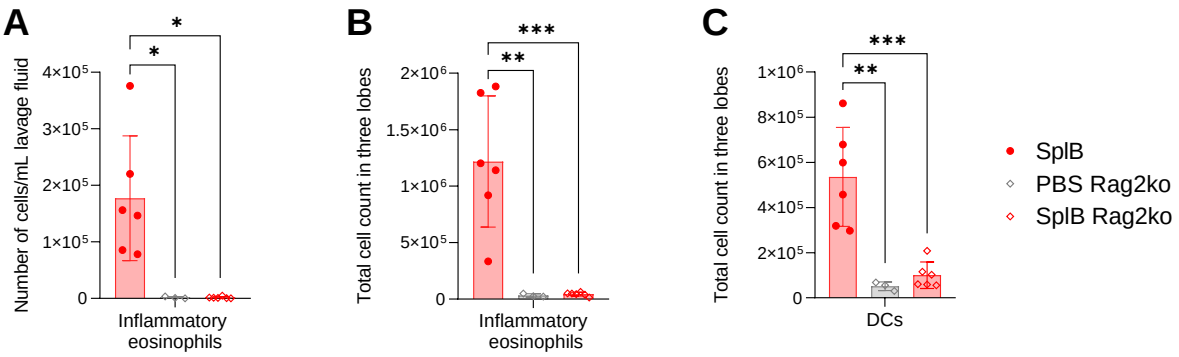

Figure 3

BAL

Lung

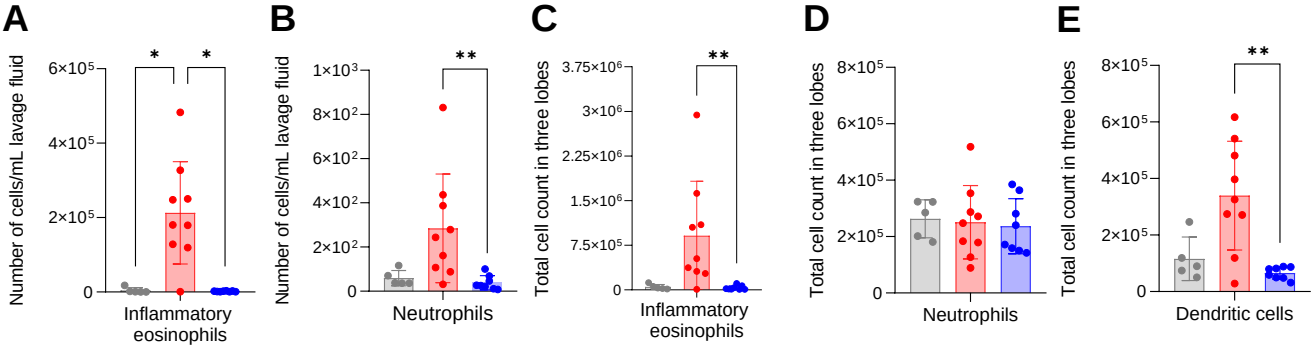

Spleen

BAL

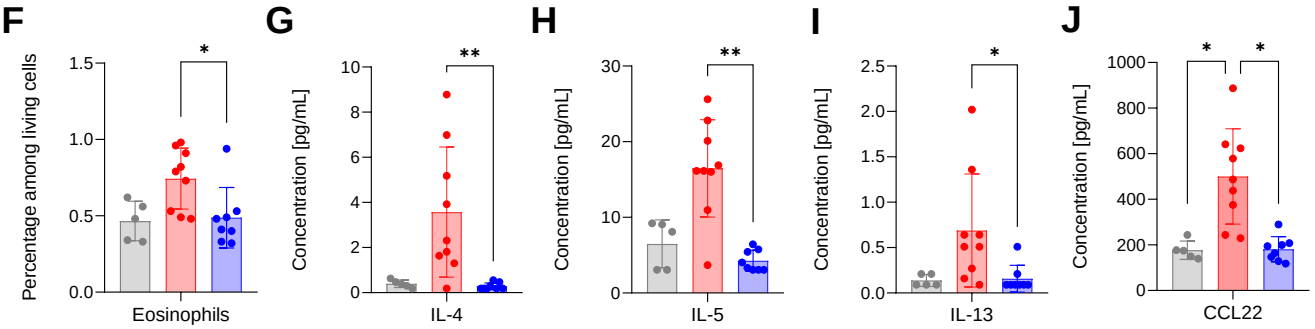

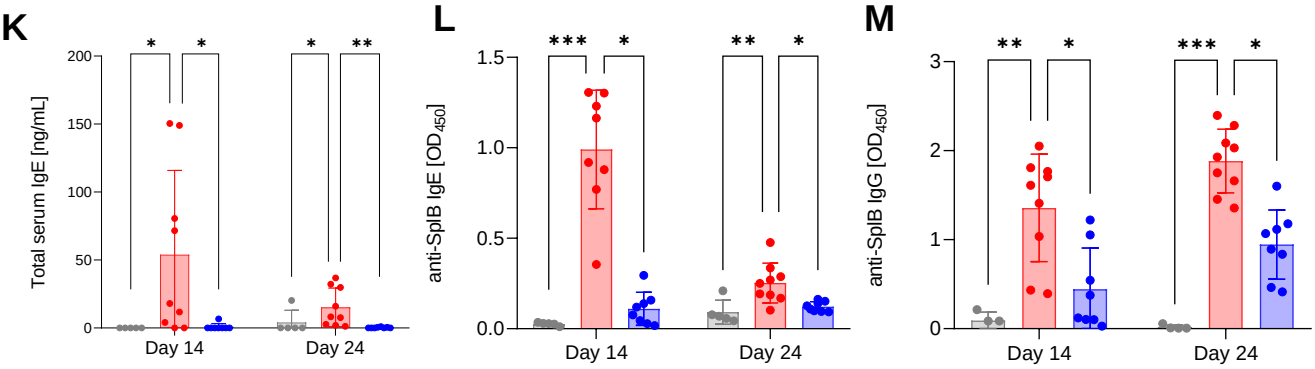

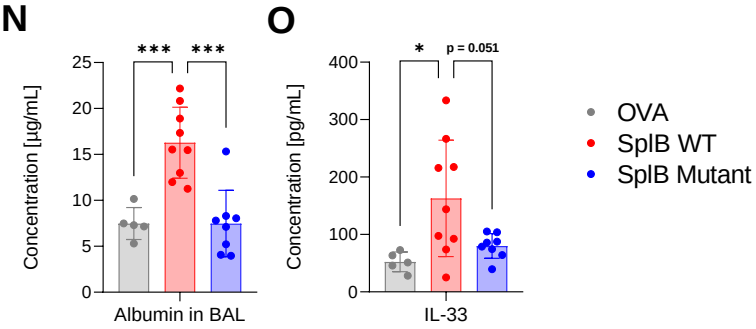

Figure 4

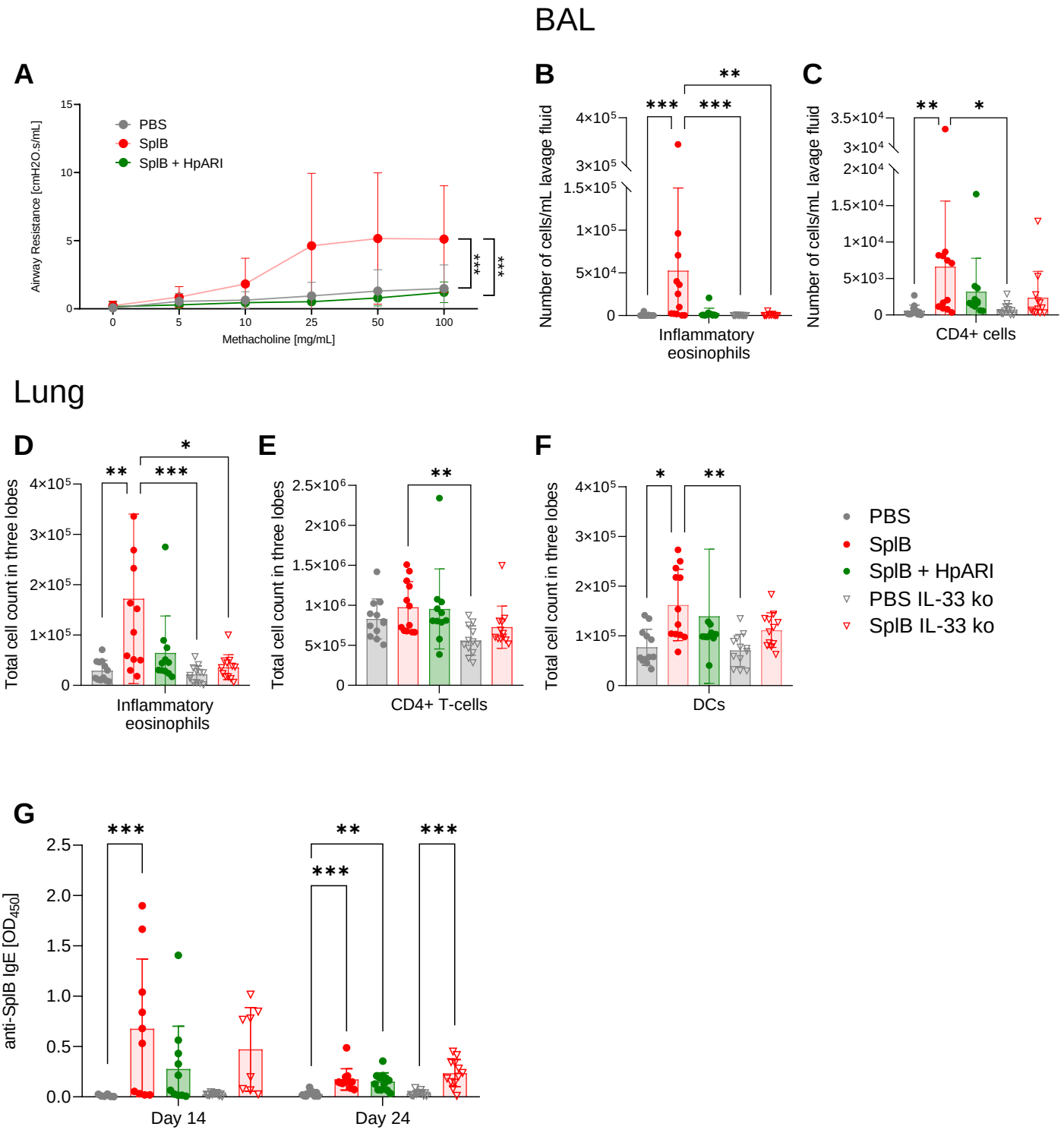
BAL
A
Airway Resistance [cmH2O.s/mL]
Methacholine [mg/mL]
PBS
SplB
SplB + HpARI
B
Number of cells/mL lavage fluid
Inflammatory eosinophils
C
Number of cells/mL lavage fluid
CD4+ cells
Lung
D
Total cell count in three lobes
Inflammatory eosinophils
E
Total cell count in three lobes
CD4+ T-cells
F
Total cell count in three lobes
DCs
PBS
SplB
SplB + HpARI
PBS IL-33 ko
SplB IL-33 ko
G
anti-SplB IgE [OD450]
Day 14
Day 24

Figure 5

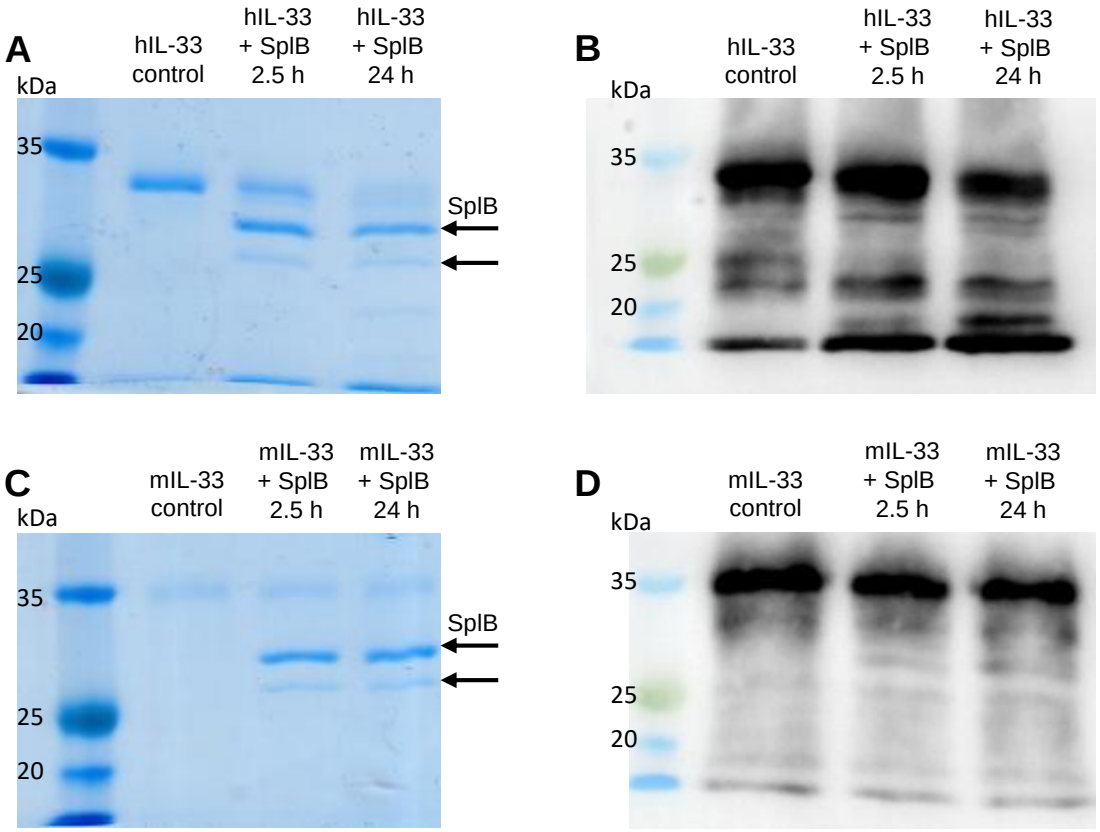
A
hIL-33 control
hIL-33 + SplB 2.5 h
hIL-33 + SplB 24 h
kDa
35
25
20
SplB
B
hIL-33 control
hIL-33 + SplB 2.5 h
hIL-33 + SplB 24 h
kDa
35
25
20
C
mIL-33 control
mIL-33 + SplB 2.5 h
mIL-33 + SplB 24 h
kDa
35
25
20
SplB
D
mIL-33 control
mIL-33 + SplB 2.5 h
mIL-33 + SplB 24 h
kDa
35
25
20

Figure 6

BAL
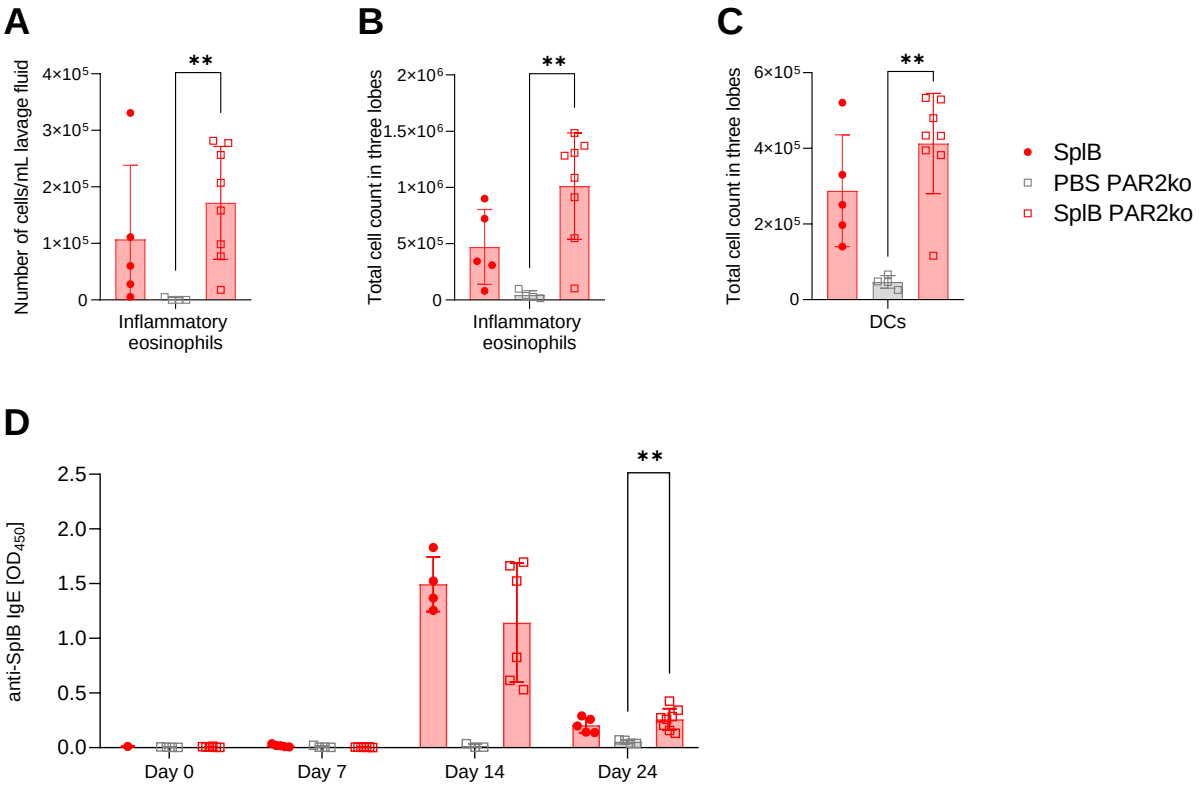
Lung